1. Introduction

Thermal input to optoelectronic devices is frequently identified as a factor that can impede performance. It is well documented that thermal input can lead to significant alterations and failures in electronic devices, as evidenced by numerous studies [1], [2]. Consequently, significant research has been conducted to limit the heat input to a device, enhance the heat transport from the device, or improve its resilience to temperature increases [3], [4], [5]. In the scenario of laser-emitting devices in general, and laser diodes especially, the thermal impact on numerous device designs has been studied extensively [6], [7], [8]. Despite its reputation, this work investigates ways to turn the drawbacks of thermal input into a semiconductor device in the opposite direction and to find concepts that allow further functionalities in the context of active optical elements. Instead of avoiding thermal input, precisely tuned heat load portions are used to alter the optical landscape within a light emitter.

The path light takes within any medium is primarily affected by the refractive index, n, of the medium it traverses. Following the principle of Fermat, the light may be diffracted, reflected, or travel along bent paths. Depending on the initial conditions, such as the shape of the light, one may use a refractive index distribution that tailors the light to specific needs. A variety of concepts exist that may be used to generate an arbitrary refractive index distribution. Approaches like proton bombardment, laser-pulse writing, or localized material diffusion are commonly applied [9], [10], [11]. The alterations introduced in this manner are time-invariant, forming a constant refractive index profile that light encounters as it passes through a potential optical device. While this behavior is expected and desired for many applications, the demand for variable optical elements is increasing. A prominent example of this development is found in photonic integrated circuits, with an ever-increasing functional density [12], where various kinds of switchable optical elements are introduced [13], [14]. However, typical variable optical elements support the transition between or the transport within predefined optical waveguides; they do not directly guide or steer the light by their input. In this work, switchable elements are presented that can address demanding challenges, such as waveguiding when switched on and then vanishing from the refractive index landscape when not needed.

Founded on GaAs-based edge-emitting devices, micro-heating elements that allow localized heat deposition are introduced. Through the well-explored thermo-optical effect, a temperature increase leads to a manipulation of the refractive index [15], affecting light propagation. In the two main parts of this thesis, the capabilities of thermo-optic elements are investigated within optical passive and active devices. The passive devices show neither optical gain nor significant losses and are used to derive fundamental properties of light propagation influenced by thermal impact. The second part introduces heating elements to active devices. Here, a typical high-power semiconductor vertical structure is applied that can be driven by an electrical current to allow optical gain within the device. In both parts,

experimental and simulation analyses are provided. The simulation is based on a tailored multi-physics model that allows the investigation of microscopic optical behavior within the devices.

This thesis is organized as follows: The Chapters 2 and 3 provide the theoretical baseline and the concept of the utilized simulation algorithm. The measurement setup is introduced in Chapter 4. In Chapter 5, devices with passive vertical structures are investigated, focusing on fundamental thermal waveguiding phenomena. In Chapter 6, micro heaters are introduced to an active vertical structure. Here, the spatial modulation of light within the device is presented. The effects of beam steering and astigmatism variation are explained in detail. This work concludes with an outlook section, exploring possible applications based on microheater elements. Additional relations and measurements are found in the appendix.

2. Theory and fundamental concepts

This work investigates the fundamental and applied aspects of thermo-optical light modulation within semiconductor-based devices. To analyze the phenomena involved, the necessary fundamentals for describing these processes are introduced. Initially, the concept of wave optics is presented as a universal tool for describing micro-optical behavior. Based on the principles of wave optics, the concept of light guiding within optical modes is presented. This is followed by a brief summary of the aspects of semiconductor-based light emission and amplification. Finally, the mechano-optical and thermo-optical effects are introduced. Both effects are the main factors influencing the optical propagation in the devices investigated here.

2.1. Wave optics and optical waveguiding

This chapter establishes the fundamental relationships that enable the description of light within optical waveguides. The characterization of optical waveguides can be approached through various methodologies. A standard method is the geometrical approach, which models light distribution as rays that travel independently within an optical system. This approach is particularly effective in describing scenarios such as multimode fiber coupling and guiding. Although the foundational principles of this concept are well-established and thoroughly explored [16], it continues to be an area of active research [17]. The geometrical approach proves to be accurate in many scenarios, even though it disregards the wave-like nature of light. However, a different approach is required for specific applications, particularly when light is confined to narrow spatial geometries. The following sections derive the fundamentals of wave optics, providing a framework for describing edge-emitting devices with longitudinally varying layouts. The classical description of an electromagnetic field follows the Maxwell's equations. Restricted to non-magnetizable materials and without electrical source or drain they can be written as

$$\nabla \times \mathbf{E} = -\mu_0 \partial_t \mathbf{H}, \tag{2.1}$$

$$\nabla \times \mathbf{H} = \mathbf{j} + \partial_t \mathbf{D}, \tag{2.2}$$

$$\nabla \cdot \mathbf{D} = 0, \tag{2.3}$$

$$\nabla \cdot \mathbf{H} = 0, \tag{2.4}$$

with the time and space dependent parameters electrical field $\mathbf{E}$, magnetic field $\mathbf{H}$, electrical current density $\mathbf{j}$ and electrical displacement field $\mathbf{D}$ and the vacuum permeability μ_0. The material response to an electrical field is given by

$$\mathbf{D} = \epsilon_0 \mathbf{E} + \mathbf{P}, \tag{2.5}$$

with the polarization density $\mathbf{P}$ and vacuum permittivity ϵ_0. The given equations are sufficient to describe arbitrary electromagnetic field distributions. However, for practical scenarios, a form, directly exhibiting the wave nature of electromagnetic radiation is preferred. To extract the wave equation concerning the electrical field one applies the curl operator to equations 2.1 and 2.2, eliminating the $\mathbf{H}$ dependency. With equation 2.3, equation 2.5 and the vector identity $\nabla \times \nabla \mathbf{E} = \nabla (\nabla \cdot \mathbf{E}) - \nabla^2 \mathbf{E}$ one yields

$$\frac{1}{\epsilon_0} \nabla (\nabla \times \mathbf{P}) + \nabla^2 \mathbf{E} = \mu_0 \partial_t \mathbf{j} + \frac{1}{c_0^2} \partial_t^2 \mathbf{E} + \mu_0 \partial_t^2 \mathbf{P}, \tag{2.6}$$

with the speed of light c_0. The material response to an electrical field, expressed by $\mathbf{P}$, is described by the convolution

$$\mathbf{P}(t) = \epsilon_0 \int_0^\infty \chi(\tau) \mathbf{E}(t - \tau)\, dt \tag{2.7}$$

with the electrical susceptibility χ. Using the convolution theorem, the time-dependent polarization in 2.7 can be transferred in the frequency domain leading to $\mathbf{P}(\omega) = \epsilon_0 \chi(\omega) \mathbf{E} \omega$. The respective wave equation in the frequency domain is obtained by applying the Fourier differentiation rule to equation 2.7 leading to

$$\frac{1}{\epsilon_0} \nabla \left(\nabla \cdot \tilde{\mathbf{P}} \right) + \nabla^2 \tilde{\mathbf{E}} = i \omega \mu_0 \mathbf{j} - k_0^2 \tilde{\mathbf{E}} - \omega^2 \mu_0 \tilde{\mathbf{P}}, \tag{2.8}$$

with the wavenumber $k_0 = \frac{2\pi}{\lambda_0}$ and the angular frequency ω. Variables with tilde superscript represent the frequency domain variable. With equation 2.5 in frequency domain and the assumption $\sqrt{\epsilon} = n$, equation 2.8 can be given as

$$\nabla \left(\frac{\nabla n^2}{n^2} \tilde{\mathbf{E}} \right) + \nabla^2 \tilde{\mathbf{E}} = -k_0^2 n^2 \tilde{\mathbf{E}}. \tag{2.9}$$

When assuming a slow variation of n, the left-hand side term can be neglected, finally leading to

$$\nabla^2 E = -k_0^2 n^2 E, \tag{2.10}$$

known as the Helmholtz equation for inhomogeneous media. The different components of $\tilde{\mathbf{E}}$ are not coupled anymore. Thus, the components can be expressed individually via the scalar potential E. Equation 2.10 can be further simplified in the context of semiconductor edge-emitting devices, that will be treated exclusively within this work.

2.1.1. Optical waveguide modes

The Helmholtz equation 2.10 sets the baseline for light propagation within the hereafter discussed optical systems. It governs the behavior of light in arbitrary spatial refractive index distributions. Within this work, directed light propagation along a given axis is the focus of research. In the scenario of a longitudinal slowly varying refractive index landscape, the propagation is conveniently described by modes. Modes are generally solutions to the

Maxwell equations and solutions to the Helmholtz equation under the given simplifications. Especially for spatial-invariant systems, modes are a fundamental concept in the description of light propagation [18], [19].
Layouts that allow the transversal confinement and hence the longitudinal transport of light over long distances are referred to as waveguides [20]. In the ideal scenario, a waveguide exhibits a longitudinal invariant behavior. Also assuming a longitudinal invariant refractive index with $n(x, y, z) \rightarrow n(x, y)$ the electrical field can be written as

$$\mathbf{E}(x, y, z) = \mathbf{E}(m)(x, y)e^{i\beta z - i\omega t}, \tag{2.11}$$

where m is introduced as the mode order. The electrical field may oscillate in different spatial orientations. However, in many scenarios, such as slab waveguides the problem can be observed one-dimensionally allowing simplifications [21], [22]. Additionally, for laser applications, one often treats with linear polarized light [23]. The electrical field vector can then be treated as a scalar parameter. Linear polarized light is then conventionally described as TE- or TM-polarized with $\mathbf{E} = E_x$ or $\mathbf{E} = E_y$ respectively, which proves to be an accurate approximation for planar-like waveguides [24]. When inserting equation 2.11 in 2.10 and assuming TE polarization, one yields

$$\frac{1}{k_0}\frac{\partial^2 E_0(x)}{\partial x^2} + n(x)^2 E_0(x) = n_{\text{eff}}^2 E_0(x), \tag{2.12}$$

with $\beta = n_{\text{eff}} \cdot k_0$ where n_{eff} denotes the modal effective index. With n being only dependent on x a one-dimensional approach is implicated. The equation, representing an eigenvalue problem, is efficiently solved by a finite difference approach as follows.

$$\begin{aligned} \frac{1}{k_0^2} &\begin{bmatrix} -2/h^2 + k_0^2 n_1^2 & 1/h^2 & 0 & 0 & 0 & \dots \\ 1/h^2 & -2/h^2 + k_0^2 n_2^2 & 1/h^2 & 0 & 0 & \dots \\ 0 & 1/h^2 & -2/h^2 + k_0^2 n_3^2 & 1/h^2 & 0 & \dots \\ 0 & 0 & \dots & \dots & \dots & \dots \end{bmatrix} \begin{bmatrix} E_1 \\ E_2 \\ E_3 \\ \dots \end{bmatrix} \\ &= \begin{bmatrix} n_1^2 \\ n_2^2 \\ n_3^2 \\ \dots \end{bmatrix} \begin{bmatrix} E_1 \\ E_2 \\ E_3 \\ \dots \end{bmatrix} \end{aligned} \tag{2.13}$$

The parameter h depends on the simulation setup and may be chosen to be proportional to the numerical grid spacing. The solution of the eigenvalue equation returns the modal electric field distribution $E_m(x)$ and the modal refractive indices n_m. The derived field distributions describe Eigenmodes that are supported by the given refractive index profile. The longitudinal (z) behavior of the individual modes is given by their propagation constants $\beta_m = n_m \cdot k_0$. In the scenario of passive waveguides, n_m is typically positive and real-valued for relevant modes. However, scenarios for so-called radiative or leaky modes can appear, that result in complex eigenvalues [25]. In the scenario of an open waveguiding problem, with infinite transversal dimension, any arbitrary field can be represented by a superposition of individual modes [26]. Subsequently, in the closed system, as implicated by the presented finite difference approach, an arbitrary electrical field may not be fully described by modes

of the waveguide. However, the fraction of light traveling, or guided, within certain modes can be calculated with the well-known overlap integral. The 1-D overlap integral between an arbitrary field distribution and a given mode reads

$$\eta_m = \frac{|\int E(x) \cdot E_m^*(x) dx|^2}{\int |E(x)|^2 dx \cdot \int |E_m(x)^2| dx}, \tag{2.14}$$

with the modal power fraction η_m.

2.2. Semiconductor light emission and amplification

The concept of semiconductor light emission is typically based on an epitaxially grown layer stack that includes heterojunctions [27]. The junction area serves as the active region of the device. When a driving current is applied in the diode's forward direction, it generates excited charge carriers, which may form a population inversion within the active region. While spontaneous emission occurs before the onset of inversion, light amplification only happens in the inverted state of operation, where stimulated emission becomes dominant. This amplification is described as optical gain. To enhance electro-optical efficiency, specific layer combinations are employed to spatially confine charge carriers, typically in the form of quantum wells [28]. These structures enable precise tuning of the emission wavelength and efficient confinement, even at elevated operating temperatures [29]. Devices based on quantum wells can be fabricated to emit either vertically or horizontally. This work focuses on devices that emit in the epitaxial plane, known as edge emitters. Besides providing optical gain, the vertical layer stack can act as an optical slab waveguide, confining the optical field in the vertical dimension. Edge emitters can be used either as laser sources themselves or as semiconductor optical amplifiers (SOAs) that amplify laser radiation. In the SOA configuration, seed laser light is coupled into the amplifier, and the optical power is continuously amplified as it propagates through the SOA [30]. In this work, the SOAs used are based on a III-V GaAs compound semiconductor material. The emission and amplification wavelengths can be adjusted by the material composition used as active region [31], [32]. This approach enables the realization of structures emitting in the range of 620 nm to 1120 nm [33], [34]. Apart from the vertical structure, the emitter characteristics are also significantly influenced by the horizontal device layout. Depending on the intended application, emitters with transverse single mode (ridge waveguide - RW), transverse multi-mode (broad area - BA), or high-power single-mode-like (tapered - TP) functionality can be fabricated. These different layouts are typically achieved using sections featuring either index or gain guiding [35]. Index guiding is generally introduced by altering the refractive index in specific regions of the device during manufacturing, leading to configurations like ridge waveguides. Gain guiding, on the other hand, results from local electrical pumping, which causes localized charge carrier excitation and consequently increased local heating. For certain functionalities, such as reducing the optical intensity at the device facets, combinations of index- and gain-guided layouts are often employed. This is particularly common in tapered amplifiers and tapered lasers, where an initial ridge waveguide section is typically followed by a gain-guided area. A typical SOA device is sketched in figure 2.1.

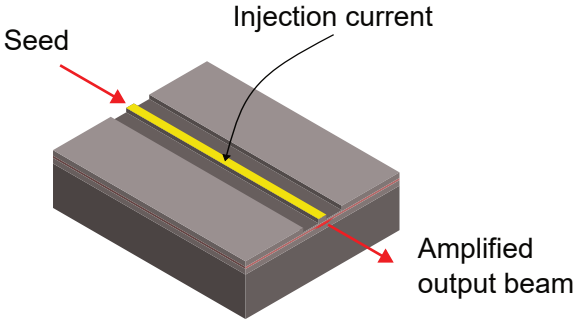

Figure 2.1.: Sketch of a tyical ridge wavguide SOA. Wavguiding in the vertical direction is introduced by the expitaxial layer stack. The horizontal waveguiding is achieved by a ridge structure. Optical amplification is achieved by the electrical pumping of the active region via the injection current.

2.3. Refractive index variation

The refractive index n is a fundamental parameter for describing the behavior of electromagnetic radiation within a medium. Generally, the refractive index is a complex quantity that accounts for both the propagation velocity of the electromagnetic wave and the medium's absorption or amplification properties. In non-magnetic materials, the refractive index is directly derived from the electromagnetic permittivity as

$$n = \sqrt{\epsilon_1 + i\epsilon_2}, \tag{2.15}$$

where ϵ_1 denotes the real part of the permittivity and ϵ_2 the imaginary part, representing the material's absorption or gain. For optically isotropic materials, the refractive index can be treated as a scalar. However, in certain cases, such as with birefringent or mechanically strained materials, the refractive index must be described using the optical indicatrix

$$n \rightarrow \mathbf{n} = \begin{bmatrix} n_{1,1} & 0 & 0 \\ 0 & n_{2,2} & 0 \\ 0 & 0 & n_{3,3} \end{bmatrix}. \tag{2.16}$$

The matrix can be visualized in the shape of an index ellipsoid. In the following sections, two effects that influence the refractive index $\mathbf{n}$ in semiconductor devices will be discussed.

2.3.1. Photoelastic effect

The introduction of mechanical stress to an optical medium is well-known for altering the refractive index. As stress is typically applied non-isotropically, a former isotropic material may exhibit a birefringent behavior [36]. The intrinsic reaction of any material to external

stress σ is its deformation, expressed as the material strain s. Stress and strain are connected via Young's modulus C with

$$C = \frac{\sigma}{s}. \tag{2.17}$$

The change in refractive index due to material deformation is called the photoelastic effect. The derivations presented hereafter follow the arguments of [37]. To calculate the impact of stress on the permittivity and refractive index, commonly a modified material equation is introduced. Instead of the permittivity, the impermeability tensor $\mathbf{B_{ij}}$ is introduced resulting in

$$\mathbf{E} = \mathbf{B_{ij}}\mathbf{D}. \tag{2.18}$$

In general, the impermeability is a tensor of second-rank. The impermeability can be linked to the material strain by the elasto-optical coefficients p_{ijrs}, which are represented by a tensor of fourth-rank. For sufficiently small material strain the relation reads

$$\Delta\mathbf{B_{ij}} = \mathbf{p}_{ijrs}s_{rs}. \tag{2.19}$$

The initial 81 entries of $\mathbf{p}_{ijrs}$ can be greatly simplified in general and especially for crystals with certain symmetries. Due to symmetry considerations, $\mathbf{p}_{ijrs}$ reduces to $\mathbf{p}_{ij}$. Also, the impermeability tensor can be simplified from $\mathbf{B_{ij}}$ to $\mathbf{B}_i$. For cubic crystals, with an initially isotropic behavior, $\mathbf{p}_{ij}$ can be simplified even further with only four independent parameters. Thus, the change in impermeability can be expressed as

$$\begin{pmatrix} \Delta B_1 \\ \Delta B_2 \\ \Delta B_3 \\ \Delta B_4 \\ \Delta B_5 \\ \Delta B_6 \end{pmatrix} = \begin{pmatrix} p_{11} & p_{12} & p_{12} & 0 & 0 & 0 \\ p_{12} & p_{11} & p_{12} & 0 & 0 & 0 \\ p_{12} & p_{13} & p_{11} & 0 & 0 & 0 \\ 0 & 0 & 0 & p_{44} & 0 & 0 \\ 0 & 0 & 0 & 0 & p_{44} & 0 \\ 0 & 0 & 0 & 0 & 0 & p_{44} \end{pmatrix} \begin{pmatrix} s_{11} \\ s_{22} \\ s_{33} \\ 2s_{23} \\ 2s_{13} \\ 2s_{12} \end{pmatrix} \tag{2.20}$$

where the strain s is noted in the Voight notation. With the individual entries, the change in refractive index can be calculated corresponding to different spatial directions. The change in permittivity can now be approximated with

$$\Delta\epsilon_{ij} \approx -\epsilon^2 \Delta B_{ij} \tag{2.21}$$

or when expressed via the refractive index

$$\Delta n_{ij} \approx \frac{-n^3}{2}\Delta B_{ij}. \tag{2.22}$$

As discussed before, this strong simplification is only valid if the impermeability tensor is isotropic before straining. Finally, the relevant entry for linearly polarized light can be selected following [38]. For TE-polarized light, where E oscillates along the x-axis the relevant refractive index is n_{11}.

2.3.2. Thermo-optical effect

The impact of temperature on optical media is a phenomenon that is evident in daily observations and an effect known for a significant period in time. While its occurrence is generally known, its description is more complex. In most scenarios, a phenomenological approach is chosen to describes the optical properties under the variation of temperature. However, it is worthwhile taking a closer look at the underlying microscopic mechanisms that, in summation, affect the optical characteristics. The response of matter to electromagnetic radiation is often modeled via oscillators of different types. As with every oscillator, its behavior depends strongly on internal damping effects, the coupling from the external driving force to the oscillator, its eigenfrequency and also the external force frequency and magnitude. These effects are accumulated within the dielectric function, which describes the behavior of electrons under the influence of an external time-dependent electric field. Derived from the oscillation equation of a driven harmonic oscillator the dielectric function is given by

$$\epsilon(\omega) = 1 + E_{\mathrm{p}} \sum_{k} \frac{f_{\mathrm{cv}}(\mathbf{k})}{E_{\mathrm{cv}}^2(\mathbf{k}) - E^2} \tag{2.23}$$

where the electronic plasma energy is given by

$$E_p = \sqrt{4\pi N \hbar e^2/m}. \tag{2.24}$$

The parameters f_{cv} and E_{cv} denote the so-called oscillator strength and transition energy. The number of oscillators per volume is given by N and the photon energy is E. To model the dielectric properties of a typical semiconductor in a wider spectral range, a higher number of individual oscillators must be used [39]. However, for this reason, a single oscillator approximation can be used when describing a narrow spectral region e.g. one possible transition. With this approach, equation 2.23 simplifies to

$$\epsilon = n^2 = 1 + \frac{E_p^2}{E_g^2 - E^2} \tag{2.25}$$

where E_g is the gap energy, corresponding to the chosen transition. It is immediately apparent that the refractive index now depends on the plasma energy and the gap energy. Both show a temperature dependency that is discussed in the following.
The plasma energy varies with the number of particles per volume, resulting in

$$\frac{dE_p^2}{dT} = \frac{4\pi\hbar^2 e^2}{m} \frac{dN}{dT} = -3k_{ex}E_p^2, \tag{2.26}$$

with the material thermal expansion coefficient k_{ex}. Following the thermo-optic coefficient can be defined as

$$\frac{dn}{dT} = n_{\mathrm{T}} = \frac{n^2 - 1}{2n} \left[-3k_{\mathrm{ex}} - 2\frac{2}{E_g} \frac{dE_g}{dT} \frac{1}{1 - (E/E_g)^2} \right]. \tag{2.27}$$

With the explicit impact of the change in E_p the impact on the gap energy E_g remains to be expressed explicitly. The variation of the gap energy with temperature is a well-known effect,

that appears in numerous semiconductor devices [40]. Two main factors of influence can be found that contribute to the gap energy shift. Firstly, the material expansion correlates with the lattice constant of the semiconductor. As the lattice is expanded the overlapping of electronic wave functions is altered, leading to a change in the energetic position and shape of valence and conduction bands, thus altering the gap energy [41]. However, this effect is not sufficient to describe the magnitude of change. The second contribution is introduced by phonon-electron interaction. It is shown, that a non-zero mean-square displacement of individual atoms alters the band structure. The magnitude of change is then proportional to the Debye-Waller factor [42].
While the theoretical basics of phonon interaction help to understand the thermo-optical effect, it proves difficult to apply the model for practical applications [40]. Therefore, the variation of $\left(\frac{\partial E_g}{\partial T}\right)_V$ can be approximated by a phenomenological approach. The concept introduced by Varshni [43] gives a robust and often utilized tool. The temperature-dependent gap energy is expressed by

$$E_g(T) = E_0 - \frac{\alpha T^2}{T + \beta}, \tag{2.28}$$

with the gap energy $E_0 = E_g(0\,\mathrm{K})$ and the constants α and β.
With equation 2.27 and 2.28 experimentally derived data can be fitted to find the unknown parameters α and β [15].
As this work focuses on GaAs-based devices, it is worth taking a closer look at equation 2.27 in the context of direction-dependent behavior. The variables E and E_p do not have spatial dependencies. In contrast, the thermal expansion expressed by k_{ex} is a material-specific parameter that is in general anisotropic due to the anisotropy nature of many crystal structures [44]. However, in the specific case of cubic crystal systems, an isotropic behavior governs the expansion behavior. Hence, for GaAs $k_{ex,[100]} = k_{ex,[010]} = k_{ex,[001]}$ holds. Therefore, the thermally introduced refractive index variation can be treated as a scalar change to the undisturbed system.

2.4. Characteristic beam parameters

An optical beam can be described by its electric field distribution, **E**. From this electric field, various parameters related to the originating beam can be derived, which is particularly useful in optical simulations. In such simulations, the electric field can be calculated at arbitrary positions within or outside an optical device. Additionally, knowing the initial electric field distribution allows one to compute the evolution of the field as it propagates through different optical elements. In this section, the calculation of parameteres that are relevant to this work are presented. For the specific case of edge-emitting devices, certain simplifications can be made before performing these calculations. Edge-emitting devices have a characteristic shape of light propagation, both within and exiting the devices. As described in section 2.2, light within an edge emitter is always guided in the vertical direction. Typically, the vertical waveguide supports only a single vertical mode. Because the vertical structure remains largely unchanged throughout the device, spatial variations in the vertical electric field can be neglected. Thus, the transverse electric field distribution at a